

# LIMITATIONS IN THE EXTRAPOLATION OF WAVE FIELDS FROM CIRCULAR MEASUREMENTS

A. Kuntz, R. Rabenstein

Multimedia Communications and Signal Processing  
Univ. Erlangen-Nuremberg, 91058 Erlangen, Germany  
phone: (+049) 9131 8527105, fax: (+049) 9131 8528849, email: {kuntz.rabe}@lnt.de  
web: www.lnt.de/LMS

## ABSTRACT

*This paper analyzes the constraints in extrapolating sound fields from measurements using circular microphone setups. Different representations of 2D wave fields are compared and several derivations for the decomposition into circular harmonics are summarized. Theoretical limits are derived for the order of the obtainable circular harmonic components due to spatial sampling, the measuring radius, and sensor noise. The consequences of order limitations are addressed for the extrapolation of wave fields to different radii. It is shown that even though an exact extrapolation is only possible within the measuring aperture, a coarse extrapolation can be possible beyond the radius of the microphone setup depending on the direction relative to the wave propagation. For this purpose far field approximations are derived for the extrapolation of an order limited decomposition of a plane wave in different directions. Real world measurements show good agreement with these investigations.*

## 1. INTRODUCTION

The acoustic performance of listening rooms in general is a trade-off between the effort for acoustic treatment and sound quality. An analysis of the sound field in the room can provide valuable information where unwanted reflections emerge from. Then, acoustic treatment at the precise positions is possible without the risk of performing unnecessary measures which could cause high installation efforts and running costs.

However, also the measurement effort for the wave field analysis rises for increasing measuring apertures that are necessary for the analysis of large regions of interest. In this paper we study approaches to sound field analysis based on circular measurements extending the theory for the extrapolation of sound fields beyond the measuring aperture: In Sec. 2 we give a short overview of several representations of acoustic wave fields and discuss their particular benefits and drawbacks. In Sec. 3 different possibilities to obtain a circular harmonic decomposition of a wave field from circular measurements are compared. Discretization errors and other limitations are discussed and their consequences for the extrapolation of wave fields beyond the measuring aperture are addressed for different directions relative to the wave propagation. Sec. 4 demonstrates the application of the findings to real world measurements.

## 2. REPRESENTATIONS OF 2D WAVE FIELDS

The task underlying the measurements used for this paper was to draw conclusions about the acoustic properties in a horizontal listening area. Therefore, the investigations are restricted to 2D wave fields, i. e. 3D fields that do not vary over the vertical axis  $z$ . For our wave field analysis we are interested in the sound pressure distribution in the whole horizontal plane at any point in time. This analysis can be performed using different representations of the sound fields of interest. Several possibilities are discussed in the following.

### 2.1 Multidimensional (MD) signals

MD signals are the most straightforward representation of any sound field. For every point of interest a microphone has to be

positioned to measure the sound pressure at this point. There is no transformation of the measured data involved, i. e. there are no errors and artifacts as in the decomposed and extrapolated representations described below. Severe drawbacks are the huge number of measuring positions and the large amount of measured data that render this approach impracticable in many cases. A possibility to perform wave field analysis with a subset of all possible positions in the horizontal plane is described in [3].

### 2.2 Multichannel (MCH) impulse responses

Room impulse responses measured e. g. on every point of the boundary surrounding the area of interest provide information on the wave field inside (Helmholtz integral [12]). As the measured data of each channel is relative to the position of the microphone of this channel, MCH impulse responses are not very intuitive to study room acoustics, especially when curved microphone setups are involved. It is not possible to read out the pressure distribution directly at any position from this representation. The extrapolation necessary to calculate the sound pressure at any point involves integrals that depend on the measuring geometry. The following wave field description avoids this problem by relating all data to one reference point independent of the geometry.

### 2.3 Circular harmonic decomposition, CHD

Wave fields can be decomposed into circular harmonics  $\tilde{P}_v(\omega)$  starting e. g. from MD measurements or MCH impulse responses. Circular harmonics are the eigenfunctions of 2D wave fields in polar coordinates and can be seen as the special case of cylindrical harmonics [12] for 2D fields

$$P_p(r, \alpha, \omega) = \sum_{v=-\infty}^{\infty} \tilde{P}_v(\omega) J_v(kr) e^{iv\alpha}. \quad (1)$$

In this equation  $J_v(x)$  denotes the Bessel function of the first kind of order  $v$  and  $k = \omega/c$  denotes the wave number. The subscript  $p$  marks signals in polar coordinates throughout this paper. The harmonic components  $\tilde{P}_v$  of the decomposed field are all relative to the coordinate origin and are independent of the radius. Circular decomposed wave fields can easily be extrapolated to positions where no microphone was set up during the measurements. It is also possible to calculate a plane wave decomposition of the wave field from the CHD [5].

### 2.4 Extrapolated wave fields

If the pressure distribution inside the whole area of interest needs to be known but a full MD measurement is impossible, the other sound field representations described above can be used. They all contain – except for measurement errors – the full information about the whole sound field as they all are parametrized representations of arbitrary wave fields. Therefore the wave field can be extrapolated to the whole area of interest from any of these descriptions within the limits described below.

However, extrapolations from CHDs are particularly easy to perform as they are independent of the measurement geometry once the decomposition is calculated. They only involve applying Eq. (1) for any point. The same argument holds for plane wave decomposed fields.

The term extrapolation is used in this context in a slightly different way than usually in signal theory. There, interpolation and extrapolation mean the reconstruction of a function from its samples, either within a sampled interval or outside of such an interval. Here, extrapolation means the reconstruction of a propagating wave from its samples in time and space. Extrapolation of waves requires not only the sample values, but also a propagation model. This model is given here by the acoustic wave equation from which Eq. (1) is derived.

### 3. CIRCULAR HARMONIC DECOMPOSITION AND EXTRAPOLATION OF WAVE FIELDS

There are several possibilities to arrive at a CHD of a 2D sound field. They will be compared in this section followed by an analysis of limiting effects in the decomposition and extrapolation of wave fields when using circular measurements.

#### 3.1 Wave field decomposition from circular measurements

The full MD measurements for wave field analysis as mentioned above can be used for any 2D pressure distribution but cause very high efforts. As we are dealing with a special class of 2D signals here, i. e. wave fields, boundary measurements are sufficient. Therefore a practical approach to wave field analysis is to use circular measurements that can be performed conveniently using a rotating microphone setup followed by a CHD of the data.

The following list summarizes several derivations of the CHD based on circular measurements:

1. Only one type of microphones ( $P_p$  or  $V_{n,p}$ ):

This derivation of the CHD starts from circular measurements of the pressure  $P_p(r_M, \alpha, \omega)$  or radial particle velocity  $V_{n,p}(r_M, \alpha, \omega)$  for radius  $r_M$ . The measured data is a  $2\pi$ -periodic signal over the angle  $\alpha$ . Therefore it is possible to calculate the Fourier series (FS) coefficients  $\hat{P}_v(r_M, \omega)$  for the pressure signal  $P_p(r_M, \alpha, \omega)$ . For the sake of clarity we omit the frequency variable  $\omega$  in the remainder

$$\hat{P}_v(r_M) = \frac{1}{2\pi} \int_0^{2\pi} P_p(r_M, \alpha') e^{-jv\alpha'} d\alpha', \quad v \in \mathbb{Z}. \quad (2)$$

Similarly, the FS for velocity measurements  $V_{n,p}$  results in

$$\hat{V}_{n,v}(r_M) = \frac{1}{2\pi} \int_0^{2\pi} V_{n,p}(r_M, \alpha') e^{-jv\alpha'} d\alpha', \quad v \in \mathbb{Z}. \quad (3)$$

The CHD can then be calculated from the FS coefficients  $\hat{P}_v(r_M)$  or  $\hat{V}_{n,v}(r_M)$  as [10]

$$\tilde{P}_v = \frac{1}{J_v(kr_M)} \hat{P}_v(r_M) = \frac{-jcp_0}{J_v(kr_M)} \hat{V}_{n,v}(r_M). \quad (4)$$

This approach causes the least measurement effort. But there are zeros in the Bessel function (and in its derivative, resp.) that restrict the usable frequency range to frequency bands without Bessel zeros because of Eq. (4).

The following modifications avoid these Bessel zeros in the denominator. The same principles are often applied in spherical microphone array processing [8].

2. Rigid scatterer:

Using a cylindrical scatterer inside the measurement setup replaces the Bessel function (or its derivative) in the denominator with a term that does not contain zeros [10].

3. Two types of microphones:

Using two types of microphones (e. g.  $P_p$  and  $V_{n,p}$ ) at the same measuring positions, it is possible to perform CHDs without scatterer and without divisions by zero. It is also possible to distinguish incoming and outgoing waves [5].

4. Cardioid microphone:

This method is similar to approach number 3, but only one microphone type is needed. There is no possibility to distinguish incoming and outgoing waves [4, 10, 7].

5. Two radii:

This approach is similar to the two microphone approach, but uses measurements on at least two radii instead of two types of microphones.

#### 3.2 Limitations in wave field analysis and extrapolation using circular measurements

When measuring sound fields, discrete microphone positions have to be used, i. e. spatial sampling of the sound field data is performed. Together with additional restrictions, this leads to limitations that have to be taken into account when decomposing and extrapolating sound fields. These limitations are discussed in this section for the concept of circular pressure measurements according to Eqs. (2), (4). Similar considerations hold for the modified approaches listed above.

##### 3.2.1 Aliasing

Due to spatial sampling, spatial aliasing can occur. In the case of circular measurements, sampling causes an infinite repetition of the Fourier series coefficients  $\hat{P}_v$  and the spherical harmonics  $\tilde{P}_v$ , respectively.

Considering the Fourier series, Eq. (2), sampling  $P_p(r_M, \alpha)$  at  $N$  points on the circle leads to the approximation

$$\hat{P}_v(r_M) \approx \hat{P}_v(r_M) = \frac{1}{2\pi} \sum_{n=0}^{N-1} P_p(r_M, \alpha_n) e^{-jv\alpha_n} \Delta\alpha_n \quad (5)$$

which can be rewritten as DFT if the measuring points are distributed equally around the circle. Therefore, only  $N$  different values for  $\hat{P}_v$  can be obtained and modal repetitions will occur at  $v = mN \forall m \in \mathbb{Z}$ .

With the exception of some very special cases, all sound fields contain an unlimited number of harmonic components. E. g. a Dirac shaped plane wave (direction  $\alpha_0$ ) can be decomposed into

$$\hat{P}_v(r) = j^{-v} J_v(kr) e^{-jv\alpha_0}, \quad v \in \mathbb{Z} \quad (6)$$

with an unlimited number of modes  $v$  [2]. Because of the characteristics of the Bessel function,  $J_v(kr)$ ,

$$\hat{P}_v(r_M) \approx 0 \quad \text{for } |v| > kr_M. \quad (7)$$

Real world wave fields in general show the same behavior. Therefore the inevitable modal aliasing will cause small errors for  $kr_M < N - |v|$  and large errors for  $kr_M > N - |v|$ .

This behavior is clearly visible in Fig. 1 for the example of  $N = 100$  measurement points. Aliasing restricts the usable harmonic components to  $|v| \leq v_{\max} = N - kr_M$ , i. e. the number of usable modes decreases due to aliasing for high frequencies  $f = kc/(2\pi)$ , marked as ❶. In Fig. 1 also the applicability of Eq. (7) to arbitrary measured fields can be observed.

As only  $N$  different values for  $\hat{P}_v$  can be calculated from  $N$  spatial samples, we can now limit our anti-aliasing considerations to  $|v| < N/2$  (❷) and specify an anti-aliasing condition for these modes:

$$kr_M < \frac{N}{2} \Rightarrow \hat{P}_v(r_M) \approx \hat{P}_v(r_M) \quad \forall |v| < \frac{N}{2} \quad (8)$$

which leads to  $f < f_{\text{al}} = 3.7$  kHz in the example shown in Fig. 1. Discussions about modal aliasing in the context of different spatio-temporal sampling schemes can be found in [1, 9].

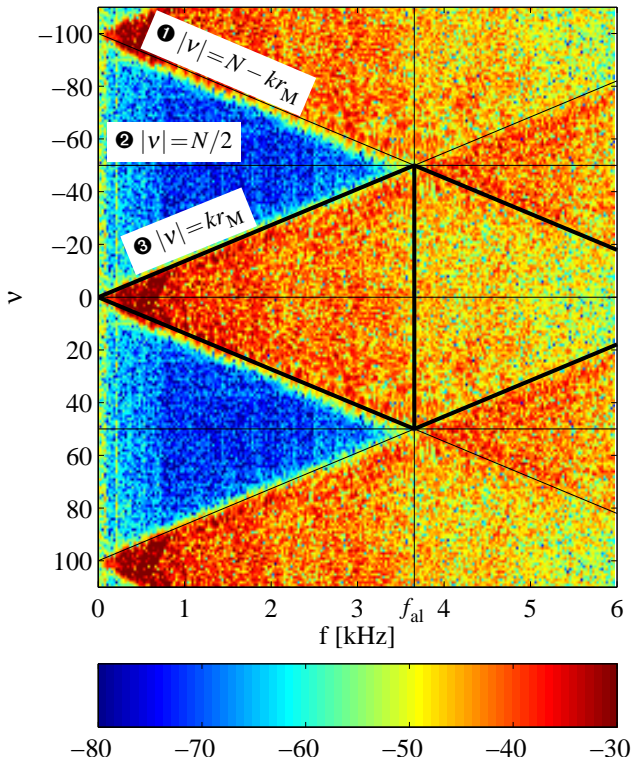


Figure 1: Magnitude of Fourier series  $\hat{P}_v(r_M, \omega)$  of discrete circular pressure measurement in dB.  $N = 100$  equispaced microphone positions with radius  $r_M = 0.74$  m were used. **1**, **2**, **3** indicate the order limits as described in the text.

### 3.2.2 Aperture limitations

Given a fixed measuring radius  $r_M$  and number of spatial samples  $N$ , a high number of harmonic components can be determined in theory, provided that the number of measuring positions  $N$  is high enough to avoid large aliasing errors. In practice, due to the sensor noise and microphone positioning errors, the number of usable harmonics is limited: Recalling Eq. (7) only the components  $|v| \lesssim kr_M$  can be used for a given  $kr_M$  because only these have a significant magnitude  $\hat{P}_v(r_M) \gg 0$  that does not get lost in the signal errors due to aliasing, sensor noise and positioning errors. This limitation is marked as **3** in Fig. 1.

### 3.2.3 2D measurements in a 3D world

In real world measurements our restriction to 2D causes two additional errors when measuring 3D fields with variations along the  $z$  axis:

- In the analysis step (decomposition), vertical components of traveling waves spread over all 2D components.
- In the extrapolation step, amplitude errors occur for 3D sources that are not line sources parallel to the  $z$  axis. The amplitude errors can be compensated for if the sources are known to be point sources.

### 3.2.4 Consequences of order limiting

Summarizing, due to the limitations **1**, **2**, and **3** described above not all harmonic components can be obtained. Depending on the measuring aperture  $r_M$ , signal frequency  $\omega$ , and number of spatial samples  $N$ , only harmonic components up to orders  $|v| \leq L$  can be captured:

$$L(r_M, \omega, N) = \min(kr_M, N - kr_M) \quad (9)$$

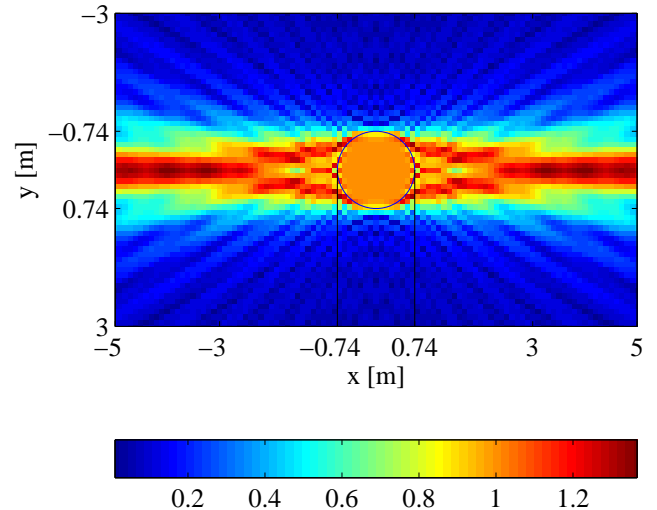


Figure 2: Magnitude of the truncated Bessel series of a monofrequent plane wave ( $f = 1.5$  kHz,  $\alpha_0 = 0^\circ$ ). The order is limited to  $|v| \leq L = 21 \approx kr_M$  for  $r_M = 0.74$  m at this frequency. Without truncation a constant magnitude of 1 is expected in the whole plane.

The modes  $|v| \leq L$  are indicated in Fig. 1 as the diamond shaped region surrounded by thick lines. If modal restrictions due to aliasing should be avoided, the triangular shaped region for  $f < f_{al}$  remains.

Now we examine the consequences of order limiting the CHD. This analysis is motivated by similar considerations for spherical harmonics shown in [6]. As an example, a truncated Jacobi-Anger series

$$P_{L,p}(r, \alpha) = \sum_{v=-L}^L \hat{P}_v(r) e^{jv\alpha}, \quad (10)$$

with  $\hat{P}_v(r)$  as in Eq. (6) is examined. It corresponds to the field of a Dirac shaped plane wave with direction  $\alpha_0$  extrapolated from a CHD limited to orders  $|v| \leq L$  (see Eqs. (1),(4),(6)).  $P_{\infty,p}(r, \alpha)$  equals the full field of a plane wave with  $|P_{\infty,p}(r, \alpha)| \equiv 1$ . Note that there is no aliasing involved in this example.

For a given value of  $L$ ,  $P_{L,p}(r, \alpha)$  is a good approximation to  $P_{\infty,p}(r, \alpha)$  if Eq. (7) holds for  $|v| > L$  which leads to  $kr < L$ . This condition defines for each frequency  $f$  a virtual aperture with radius

$$r < \frac{L}{2\pi f} c. \quad (11)$$

For a fixed  $L$  this radius  $r$  is frequency dependent. If we reconsider the frequency dependency of the order limitation due to the measurement aperture  $r_M$  when decomposing the wave field,  $L(r_M, \omega) = r_M \omega / c$ , we can substitute  $L$  in Eq. (11):

$$r < \frac{r_M \omega / c}{2\pi f} c = r_M \quad (12)$$

This equation states that the wave field can only be extrapolated without errors inside the measurement aperture with radius  $r_M$ . The correct magnitude inside the aperture is clearly visible in Fig. 2 for a monofrequent plane wave ( $f = 1.5$  kHz) and  $L = 21$ . In the implementation of the extrapolation Eq. (1) for limited orders  $|v| \leq L$ , the frequency dependency of  $L$  is undesired. One possibility to avoid a frequency dependent number of summands is to use a fixed maximum  $L$  and set the unused harmonic components equal zero.

For larger radii, i. e.  $kr > L$ , significant errors occur due to the truncation because circular harmonic components with significant

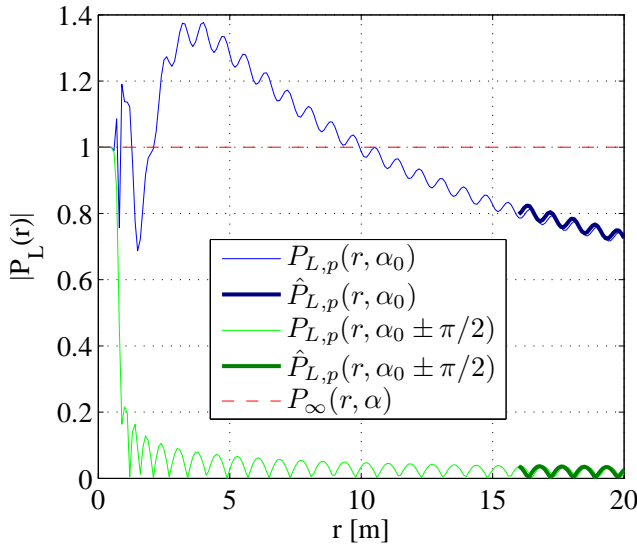


Figure 3: Magnitude of truncated Bessel series. Curves show signals of Fig. 2 for  $\alpha = \alpha_0$  and  $\alpha = \alpha_0 \pm \pi/2$ . The far field approximations Eqs. (14) and (16) are indicated as bold lines. The dashed line indicates the magnitude of the full plane wave, i.e. an infinite Bessel series.

magnitude are missing. However, depending on the application extrapolations of wave fields beyond the aperture radius can be useful as long as the limitations due to order limiting are kept in mind. These limitations will be examined in the following for two interesting cases.

The behavior of (10) for radii beyond the aperture can only be analyzed numerically. Therefore we introduce far field approximations that lead to simpler terms: For large arguments  $kr \gg |\nu^2 - 0.25|$  the Bessel functions can be approximated by [11]

$$J_\nu(kr) \approx \sqrt{\frac{2}{\pi kr}} \cos\left(kr - \frac{\nu\pi}{2} - \frac{\pi}{4}\right). \quad (13)$$

Substituting  $J_\nu(kr)$  in (10) we arrive at the following expression for the resulting field in the direction of propagation of the plane wave,  $\alpha = \alpha_0$ :

$$\begin{aligned} P_{L,p}(r, \alpha_0) &\approx \hat{P}_{L,p}(r, \alpha_0) = \\ &= \sqrt{\frac{2}{\pi kr}} \left[ (-1)^L \cos\left(kr - \frac{\pi}{4}\right) + 2 \left[\frac{L}{2}\right] e^{j\left(kr - \frac{\pi}{4}\right)} \right] \end{aligned} \quad (14)$$

For  $L \gg 1$  the cosine term can be neglected and due to the second term in the brackets an amplitude of

$$|\hat{P}_{L,p}(r, \alpha_0)| \approx L \cdot \sqrt{\frac{2}{(\pi kr)}} \quad (15)$$

remains. Substituting  $kr$  by the limit for the Bessel approximation  $kr \approx L^2$  (see above Eq. (13)) we arrive at an amplitude of  $|\hat{P}_{L,p}(L^2/k, \alpha_0)| \approx 0.8$ .

The magnitude of the truncated Bessel series, the far field approximation, and a full plane wave field are shown in the upper curves of Fig. 3 for  $\alpha = \alpha_0$ . In consequence equation (14) states that a coarse estimation of the wave field outside the measurement aperture is possible in the direction of wave propagation by extrapolating the order limited decomposition. In the far field an amplitude error proportional to  $1/\sqrt{kr}$  has to be accepted.

Orthogonal to the traveling direction of the plane wave, i.e. for  $\alpha = \alpha_0 \pm \pi/2$ , substituting Eq. (13) in Eq. (10) leads to the approximation

$$\hat{P}_{L,p}(r, \alpha_0 \pm \pi/2) = \sqrt{\frac{2}{\pi kr}} (-1)^{\lfloor \frac{L}{2} \rfloor} \cos\left(kr - \frac{\pi}{4}\right). \quad (16)$$

This expression rapidly declines for increasing  $kr$ . Thus no extrapolation of the wave field is possible in this direction. This behavior for  $\alpha = \alpha_0 \pm \pi/2$  is shown in the lower curves of Fig. 3.

Now we can summarize the consequences of order limiting when using circular measurements:

- The usable orders of the circular harmonic components are limited depending on radius  $r_M$ , frequency  $\omega$ , and order  $N$ .
- The extrapolation from the order limited CHD is possible without large errors inside the measurement aperture if enough spatial samples are used to avoid large aliasing errors.
- Outside the measurements aperture, a rough extrapolation is possible in the direction of wave propagation whereas no extrapolation is possible orthogonal to this direction.

#### 4. MEASUREMENTS AND INTERPRETATION

Room impulse responses were measured in a horizontal plane at ear level in a listening room. The measurements were performed for 100 equidistant positions  $(r_M, \alpha)$  on a circle with  $r_M = 0.74$  m for the pressure  $P_p(r_M, \alpha)$  as well as for the radial component of the particle velocity,  $V_{n,p}(r_M, \alpha)$ .

With these measurements, a discrimination between incoming and outgoing waves is possible using the CHD according to Sec. 3.1, possibility 3. With this approach numerical problems occur when extrapolating to positions near the origin that can be avoided by calculating a plane wave decomposition from the CHD first. As we are dealing with a source free region inside our measurement setup, the more direct approach number 4 of Sec. 3.1 was used with a virtual cardioid microphone formed by adding the pressure and the velocity measurements

$$C_p(r, \alpha) = P_p(r, \alpha) + \rho_0 c V_{n,p}(r, \alpha). \quad (17)$$

The Fourier series coefficients as well as the circular harmonic components were order limited according to Sec. 3.2. After the CHD, the signals were band limited to frequencies below 3.7 kHz to avoid large aliasing errors.

Fig. 4 shows the wave field extrapolated from the band limited CHD at time  $t = 17.5$  ms for extrapolation radii  $r \leq 1.8$  m. The direct sound from the acoustic source already passed the origin and the first strong reflection is arriving from  $\approx 45^\circ$ . The effects of order limiting due to the measurement aperture  $r_M = 0.74$  m can be observed as predicted in Sec. 3.2.4: Inside the aperture, the extrapolation does not cause large errors. In the direction of wave propagation, the extrapolation is also possible beyond  $r_M = 0.74$  m accepting some amplitude errors. The projection of the aperture in the direction of the direct sound propagation is indicated by the dashed lines. Orthogonal to this direction, the amplitude of the extrapolated field rapidly vanishes for  $r > 0.74$  m.

Fig. 4 indicates that at an angle of  $\approx 45^\circ$  a strong undesired reflection occurs in the listening room for the sound of the investigated source. Whether a passive or active compensation of this room reflection is necessary depends on the content that should be reproduced and the demands on the sound quality and is a matter of psychoacoustical considerations and acceptable costs for the acoustical treatment. In the Fig. 4 also additional waves are visible closely behind the wave front of the direct sound. With the background knowledge of the room geometry they can be identified as vertical sound components from reflections above the listening area.

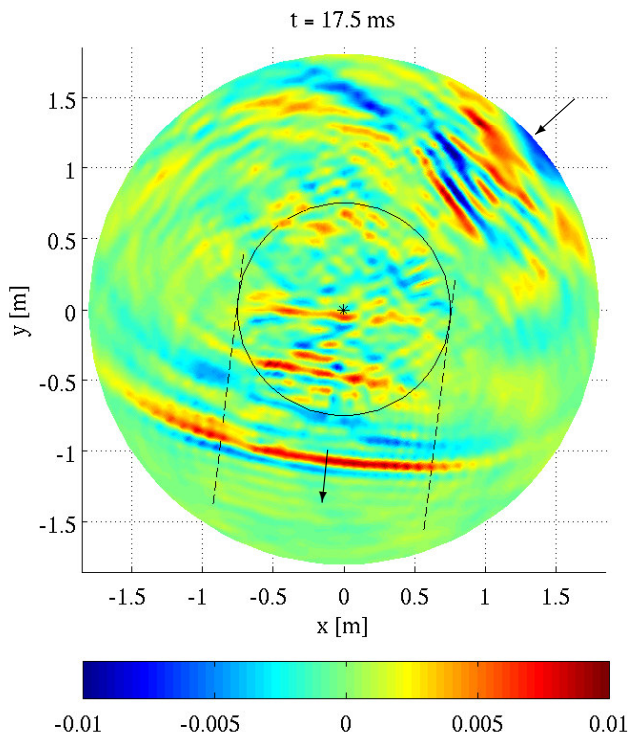


Figure 4: Extrapolated pressure distribution (linear scale) at time  $t = 17.5\text{ms}$ . The measurement aperture is indicated as a circle with  $r = 0.74\text{m}$ . The arrow inside the wave field shows the traveling direction of the direct sound wave, the arrow outside marks the traveling direction of the first strong reflection.

### 5. CONCLUSIONS

The determination of wave fields inside of enclosures is a trade-off between the number of measurement positions (microphone channels) and the resulting accuracy. Practical measurement setups consist of a number of microphones mounted on a closed curve, e.g. a line or a circle. Sequential measurements on a circular contour can be realized with very little instrumentation, since they require only one or two microphones and a computer-controlled stepper-motor drive.

The obtained measurements allow the reconstruction of the wave field not only inside the circle of measurements but also outside with the restriction to the propagation direction. The mathematical tool for this extrapolation is the decomposition of the mea-

surement values into circular harmonics. The usable orders of its components are limited by the finite radius of the measurement circle, the frequency range of the audio signals, and the finite number of measurement positions on the circle. However, a careful analysis of these restrictions allows the determination of the spatial structure of wave fields.

### REFERENCES

- [1] T. Ajdler, L. Sbaiz, and M. Vetterli. The Plenacoustic Function and its Sampling. *IEEE Transactions on Signal Processing*, 54(10):3790–3804, 2006.
- [2] I. S. Gradshteyn and I. M. Ryzhik. *Tables of Integrals, Series and Products*. Academic Press, 1965.
- [3] M. Guillaume and Y. Grenier. Sound field analysis with a two-dimensional microphone array. In *Proceedings of IEEE International Conference on Acoustics, Speech, and Signal Processing (ICASSP '06)*, Toulouse, France, May 2006.
- [4] E. Hulsebos. *Auralization using Wave Field Synthesis*. PhD thesis, Technische Universiteit Delft, 2004.
- [5] E. Hulsebos, D. de Vries, and E. Bourdillat. *Improved microphone array configurations for auralization of sound fields by Wave Field Synthesis*. preprint 5337, 110th AES Convention, Amsterdam, May 2001.
- [6] A. Ludwig. Plane and spherical wave spectra. [http://www.silcom.com/~aludwig/Physics/Exact\\_piston/Wave\\_spectra.htm](http://www.silcom.com/~aludwig/Physics/Exact_piston/Wave_spectra.htm). accessed 2007/01/31.
- [7] M. A. Poletti. A unified theory of horizontal holographic sound systems. *Journal Audio Eng. Soc.*, 48:1155–1182, 2000.
- [8] B. Rafaely. Analysis and design of spherical microphone arrays. *IEEE Transactions on Speech and Audio Processing*, 13(1):135–143, 2005.
- [9] S. Spors and R. Rabenstein. Spatial aliasing artifacts produced by linear and circular loudspeaker arrays used for wave field synthesis. In *Audio Engineering Society (AES) 120th Convention*, Paris, France, May 2006.
- [10] H. Teutsch. *Modal Array Signal Processing: Principles and Applications of Acoustic Wavefield Decomposition*. Springer, 2007.
- [11] E. W. Weisstein. Bessel function of the first kind. <http://mathworld.wolfram.com/BesselFunctionoftheFirstKind.html>. accessed 2007/02/12.
- [12] E. G. Williams. *Fourier Acoustics*. London, Academic Press, 1999.